Original Article

Early Changes during Skin Repair Using Tissue-Engineered Dermal Template in a Full-Thickness Burn

(wound healing / angiogenesis / artificial skin / tissue engineering / burn injury)

P. GÁL[1,2,3], L. FRÖHLICHOVÁ[4], M. ČOMA[2,5], I. PAFČUGA[1], H. ŠUCA[1], I. GROSSOVÁ[1], Z. HRÍBIKOVÁ[2], E. STICOVÁ[6,7], R. ZAJÍČEK[1]

[1]Prague Burn Centre, Third Faculty of Medicine, Charles University and Faculty Hospital Královské Vinohrady, Prague, Czech Republic
[2]Department of Biomedical Research, East-Slovak Institute of Cardiovascular Diseases, Inc., Košice, Slovak Republic
[3]Laboratory of Cell Interactions, Center of Clinical and Preclinical Research MediPark, Pavol Jozef Šafárik University, Košice, Slovak Republic
[4]Department of Pathology, Louis Pasteur University Hospital, Košice, Slovak Republic
[5]Department of Pharmacology, Faculty of Medicine, Pavol Jozef Šafárik University, Košice, Slovak Republic
[6]Department of Pathology, Third Faculty of Medicine, Charles University, Prague, Czech Republic
[7]Clinical and Transplant Pathology Department, Institute of Clinical and Experimental Medicine, Prague, Czech Republic

Abstract. Rapid wound closure in extensively burned patients has remained one of the major unresolved issues of medicine. Integra® is the most widely established artificial skin, which is composed of a porous matrix of cross-linked bovine collagen and chondroitin 6-sulphate covered by a semi-permeable silicone layer. We present here a (immuno)histological study of a severely burned patient with a full-thickness burn treated with a tissue-engineered dermal template (Integra®) and split-thickness skin graft-based protocol. Immunohistochemical investigation of the artificial dermis revealed that immune cell infiltration reached its peak on day 10. Tissue immunophenotyping found an increase in CD3$^+$ cells over the course of the study as well as CD4 and CD8 positivity on day 40, indicating remaining T-cell subpopulations. We observed weak/no infiltration of NK cells (CD56$^+$). In conclusion, the use of bi-layer Integra® represents a feasible and safe procedure resulting in formation of non-irritating dermal substitutes.

Received September 16, 2020. Accepted November 16, 2020.

This study was supported by Charles University (PROGRES Q37) and project implementation: Medical University Science Park in Košice (MediPark, Košice - Phase II) ITMS2014+ 313011D103 supported by the Operational Programme Research & Innovations, funded by the ERDF.

Corresponding author: Peter Gál, East-Slovak Institute of Cardiovascular Diseases and P. J. Šafárik University, (Center of Clinical and Preclinical Research MediPark), Trieda SNP 1, 040 11 Košice, Slovak Republic. Fax: +421 55 789 1610; e-mail:galovci@yahoo.com or pgal@vusch.sk

Abbreviations: SPD – *stratum papilare dermis*, STSG – split-thickness skin graft; TBSA – total body surface area; SCT – subcutaneous tissue.

Introduction

Large and deep wounds with the loss of all skin adnexa may only be healed by application of either autologous keratinocytes, epidermal grafting, or more commonly a split-thickness skin graft (STSG) (Auxenfans et al., 2015; Kanapathy et al., 2016); the depth of the injury is thus a critical parameter reflecting the ability of skin to regenerate (Dunkin et al., 2007). Although these procedures provide an adequate barrier between the outer and inner environments by restoring the epidermis, only little is done to regenerate the dermis. In particular, full-thickness burns following excision of the dead tissue, covered only with STSG, may tend to form hypertrophic scars and contractures (Varkey et al., 2015). Therefore, from the long-term perspective, defects repaired with full-thickness transplants demonstrate remarkably better functional and cosmetic appearances (Nguyen et al., 2010).

The dermal templates may be categorized as decellularized human or animal skin, artificially constructed scaffolds, or entirely synthetic polymers (Cheshire et al., 2016). Integra® is the most widely established artificial skin (Haertsch, 2002), which is composed of a porous matrix of cross-linked bovine tendon collagen and glycosaminoglycan (chondroitin 6-sulphate) obtained from

shark cartilage covered by a semi-permeable silicone layer that temporarily replaces the epidermis (Dagalakis et al., 1980; Yannas and Burke, 1980; Yannas et al., 1980, 1981; Heimbach et al., 2003). This artificial skin was developed in the Massachusetts General Hospital, Boston Shriners Burns Center and Massachusetts Institute of Technology in the late 1970s (US Patent 4,060,081A). At the beginning, it was expected that the structure of the artificial dermis would resemble normal dermis and serve as a template for synthesis of the new connective tissue while it slowly degrades (Burke et al., 1981).

In this context, several animal studies have demonstrated its ability to facilitate host cell infiltration, neoangiogenesis and deposition of endogenous collagen (Yannas et al., 1989; King et al., 1997; Grant et al., 2001; Shaterian et al., 2009; Capito et al., 2012). The first performed histological investigation conducted on 131 human subjects divided the healing process of Integra® into six phases (Stern et al., 1990). Whereas Phase I (0–7d) was never evaluated, Phases II (7–10d), III (10–15d), IV (14–17d), V (18–25d), and VI (30+d) were systematically examined for the presence of inflammatory cells, fibroblasts, sprouting vessels, collagen deposition, as well as degradation of the remaining template components and structure. Nowadays it is clear that the expected biodegradation during the neodermis formation in humans is not complete (Zajicek et al., 2018). Despite its two main limitations, the price and susceptibility to infection, the use of the template results in an excellent cosmetic and functional outcome (Nguyen et al., 2010a). In particular, the elastic properties of areas reconstructed with Integra® have been found comparable to normal skin.

Although the incomplete biodegradability of Integra® (Zajicek et al., 2018) does not clinically correlate with a negative functional outcome (Nguyen et al., 2010), the reaction of the immune system to the artificial skin has to be further elucidated to better understand its biocompatibility. Thus, we present here a case of severely burned patient treated with an Integra®/STSG-based protocol. In particular, we focused on histological examination of the early stages of Integra® remodelling during the skin repair.

Material and Methods

Human subject

The study was approved by the Ethical Committee of University Hospital Královské Vinohrady (EK-VP/04/0/2016). A thirty-nine-year-old woman was admitted due to chemical burns encompassing a total body surface area (TBSA) of 40 % with grade III involvement, from a mixture of strong acids and hydroxides (Fig. 1). This accident happened during a motor vehicle collision in which one vehicle was transporting said chemicals. The aforementioned injury completely involved the head and neck as well as the torso and limbs. In the area of the face and neck, excision was performed within 48 h. The areas were temporarily covered with biological covers (porcine skin xenograft). Bi-layer Integra® (Integra LifeSciences Corp., NJ) was applied on the neck and face on day 10 following injury. The artificial skin matured without infection or haematomas. Thirty-three days after Integra® application, the neodermis was covered with STSG removed from the patient's limbs; the STSG healed within two weeks after grafting.

Histopathology

Full-thickness punch biopsies, 3 mm in diameter, of the areas previously treated with bi-layer Integra® were systematically removed and processed routinely for histopathological examination. Samples were removed (with the informed consent of the patient) on days 7, 10, 21 and 40 following Integra® application. Briefly, specimens were fixed in 4% buffered formaldehyde, dehydrated in increasing concentrations of ethanol and embedded in paraffin. Thin, 2 μm, sections were then stained with haematoxylin-eosin (basic staining) and Sirius red (collagen staining). Firstly, immunohistochemical analysis was performed using primary antibodies (Table 1) directed against markers identifying inflammatory/immune cells (with focus on major T-cell subsets): leukocyte common antigen (LCA/CD45), CD3, CD4, CD8, CD56, CD57. Secondly, vimentin (Vim), CD31, CD34, α-smooth muscle actin (SMA), Ki67, Bcl-2, p53, p63, keratins-14 (K14) and -19 (K19), and E-cadherin (E-Cad) were immunohistochemically stained (Table 1) to score the repair process of Integra® and STSG.

Semi-quantitative analysis of immunohistological markers

A semi-quantitative method was used to evaluate the immunohistologically stained structures. Sections were examined as coded slides by two well-trained experts according to the scale: − absent, + minimal, ++ moderate, and +++ marked.

Results

Histopathology of the dermal template and STSG

Extended histological analysis using basic staining (haematoxylin-eosin), collagen staining and immunohistochemistry and the results of semi-quantitative evaluation of distinct parameters of the skin biopsies at the four time points are given in Figures (2, 3, 4 and 5) and Tables (2, 3 and 4), respectively.

On day 7, basic staining revealed porous thick (eosinophilic) fibers of the artificial dermal template that were dominantly infiltrated with inflammatory (based on cell morphology, we identified macrophages and neutrophils) cells (see Table 2, for detailed immunophenotype, see below); vimentin-expressing fibroblasts and CD31/34-positive endothelial cells (see Table 3) were also present. Vessel sprouting was rather seen from the subcuta-

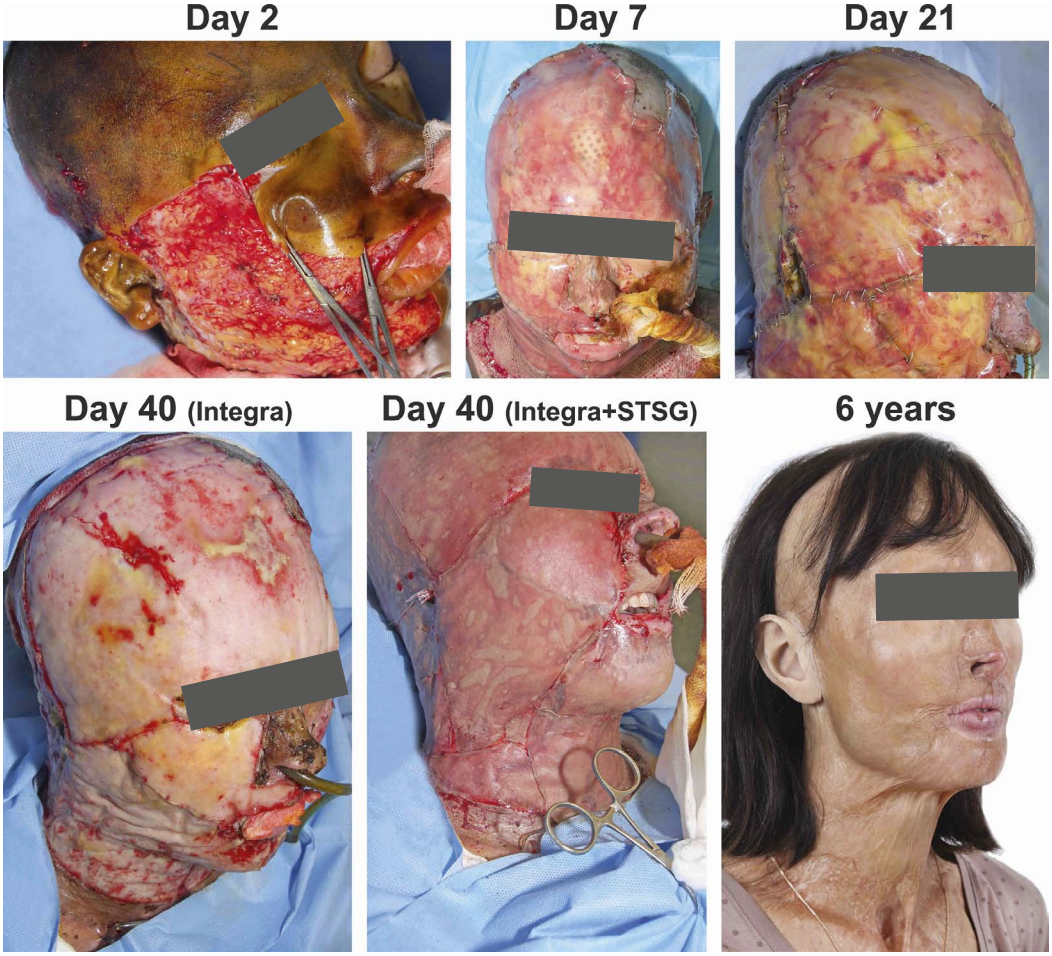

Fig. 1. Thirty-nine-year-old with full-thickness burn injury involving 40 % TBSA. Excision of full-thickness skin defects on the face on day 2 post injury. Successful Integra® application on day 7. Integra® vascularized on day 21. STSG grafted on day 40. Final outcome six years after injury.

Table 1. Reagents used for immunohistochemistry

IHC antibody (clone)	vendor/producer	dilution	pretreatment	instrument	detection system
LCA (RP2/18)	Roche Ventana	RTU	CC1 36 min	Benchmark Ultra, Ventana	HRP/DAB
CD3 (2GV6)	Roche Ventana	RTU	CC1 36 min	Benchmark Ultra, Ventana	HRP/DAB
CD4 (SP35)	CellMarque	1:100	High pH, 20 min	PTLink, manual	HRP/DAB
CD8 (917-V)	DB Biotech	1:200	High pH, 20 min	PTLink, manual	HRP/DAB
CD56 (123C3)	DAKO Agilent	RTU	High pH, 20 min	PTLink, Autostainer Link48	HRP/DAB
CD57 (NK-1)	Diagnostic Biosystems	RTU	High pH, 20 min	PTLink, manual	HRP/DAB
Vimentin (V6)	Roche Ventana	RTU	CC1 20 min	Benchmark Ultra, Ventana	HRP/DAB
CD31 (JC/70A)	Diagnostic Biosystems	RTU	CC1 64 min	Benchmark Ultra, Ventana	HRP/DAB
CD34 (QBEND/10)	Roche Ventana	RTU	CC1 20 min	Benchmark Ultra, Ventana	HRP/DAB
SMA (1A4)	DAKO Agilent	RTU	High pH, 20 min	PTLink, Autostainer Link48	HRP/DAB
Ki67 (30-9)	Roche Ventana	RTU	CC1 36 min	Benchmark Ultra, Ventana	HRP/DAB
Bcl2 (124)	DAKO Agilent	RTU	High pH, 20 min	PTLink, Autostainer Link48	HRP/DAB
p53 (DO-7)	Roche Ventana	RTU	CC1 36 min	Benchmark Ultra, Ventana	HRP/DAB
p63 (EP235)	Roche Ventana	RTU	CC1 36 min	Benchmark Ultra, Ventana	HRP/DAB
K14 (D19-N)	DB Biotech	RTU	CC1 36 min	Benchmark Ultra, Ventana	HRP/DAB
K19 (E16-L)	DB Biotech	1:100	High pH, 20 min	PTLink, manual	HRP/DAB
E-cadherin (NCH38)	DAKO Agilent	RTU	High pH, 20 min	PTLink, Autostainer Link48	HRP/DAB

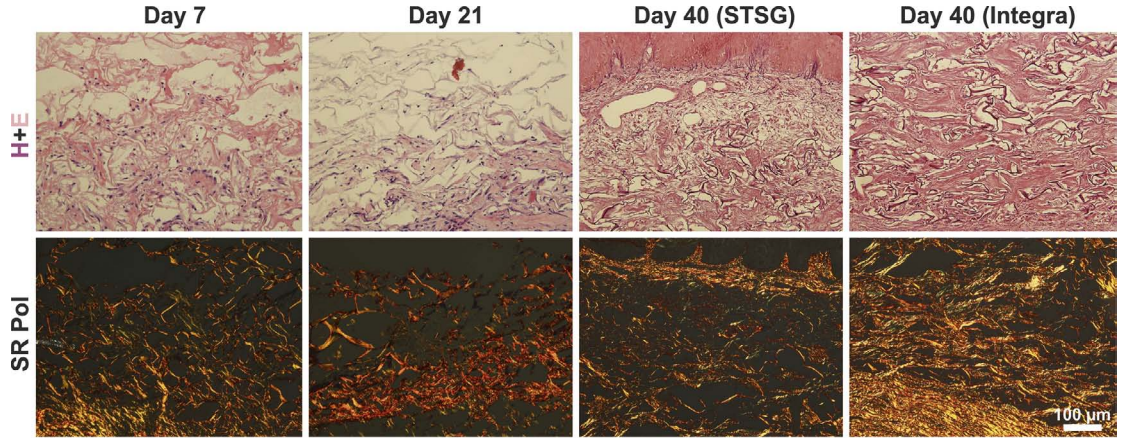

Fig. 2. Histological samples (stained with haematoxylin-eosin (H+E) and Sirius red (SR)) examined 7, 21 and 40 days after injury (magnification 200×; scale 100 µm).

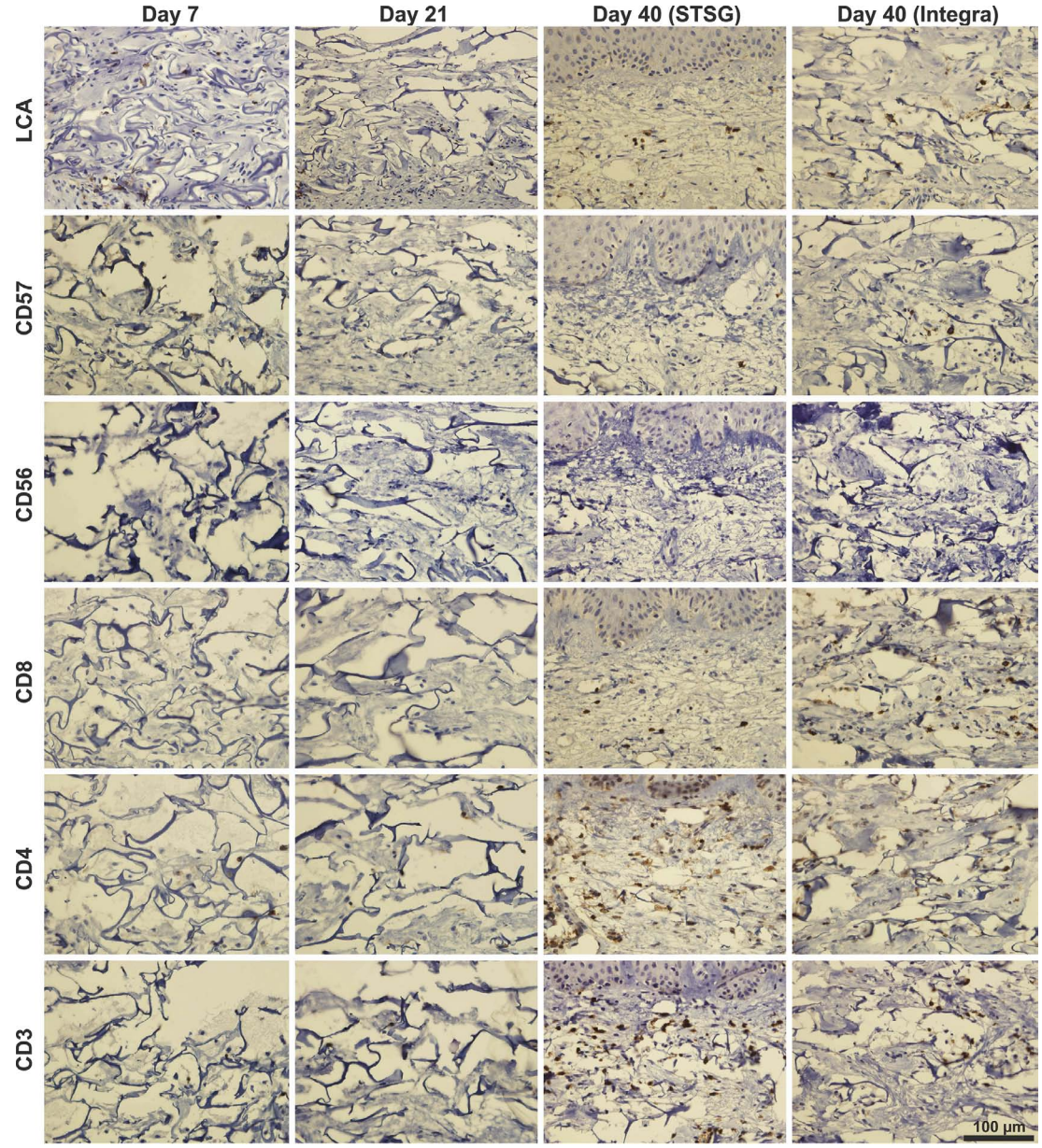

Fig. 3. Histological samples processed for immunohistochemistry examined 7, 21 and 40 days after injury (STSG – split-thickness skin graft; magnification 400×; scale 100 µm).

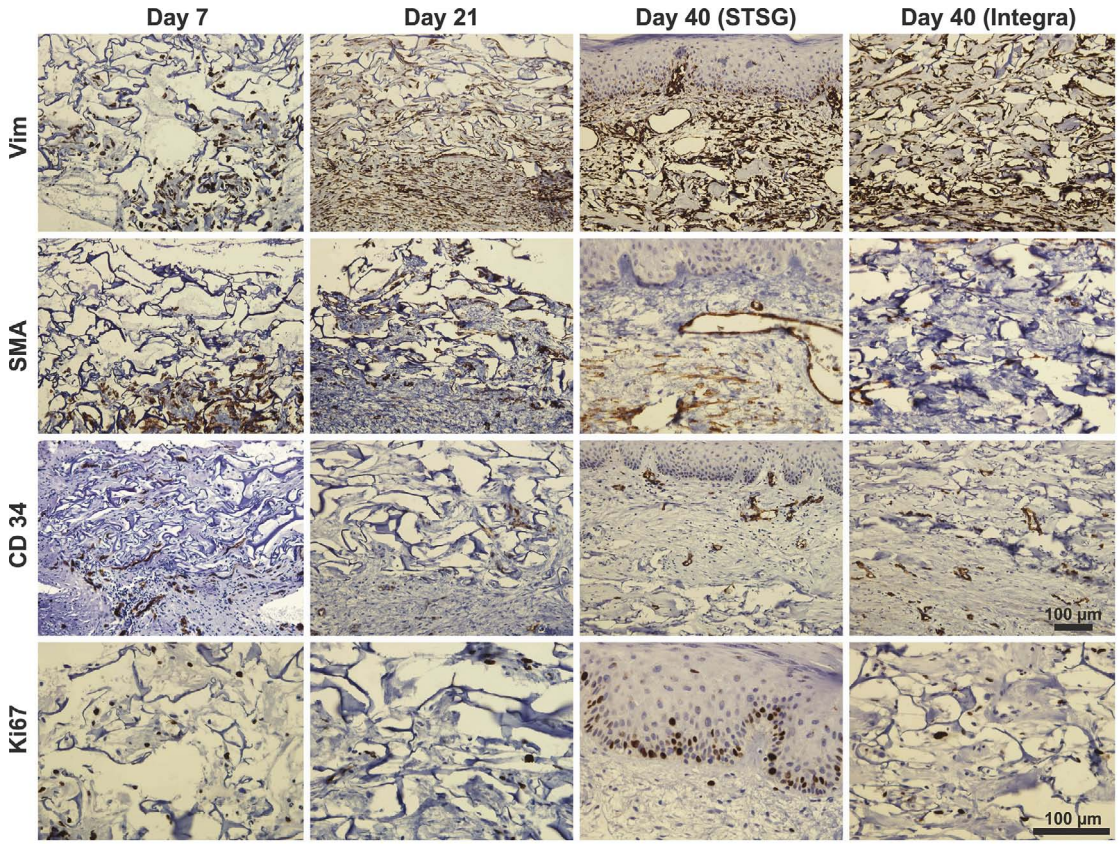

Fig. 4. Histological samples processed for immunohistochemistry examined 7, 21 and 40 days after injury (staining for Vim, SMA and CD34 – magnification 200x; staining for Ki67 – magnification 400×; scale 100 µm).

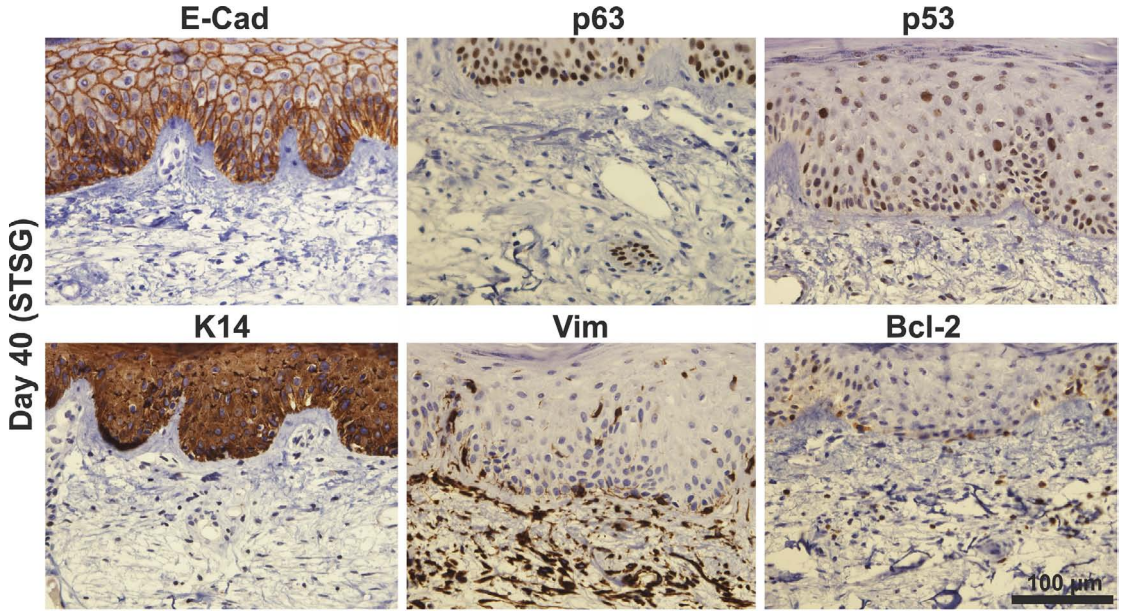

Fig. 5. Histological samples (STSG – split-thickens skin graft) processed for immunohistochemistry examined 40 days after injury (magnification 400×; scale 100 µm).

neous tissue (Fig. 3) and did not reach the middle and/or superficial portion of the template. Later, on days 21 and 40, luminized (CD31/34^{-} and SMA-positive) vessels were present throughout the whole neodermis. The presence of vimentin-expressing fibroblasts and SMA-expressing myofibroblasts gradually increased within the evaluated time intervals. From day 10 to day 21, the activity of the cells increased (cells expressed Ki67) and

Table 2. Semi-quantitative analysis of inflammatory/immune cells in bioptic samples removed from areas covered by Integra® dermal template and split-thickness skin graft (STSG)

		LCA	CD3	CD4	CD8	CD56	CD57
Integra®	Day 7	+	+/–	+/–	–	–	–
	Day 10	++	+/–	+/–	–	–	–
	Day 21	+	+/–	+	–	–	–
	Day 40	+	+	++	+	–	+/–
SCT	Day 7	++	+/–	++	+/–	–	–
	Day 10	++	+/–	++	+	–	–
	Day 21	+	+/–	+/–	–	–	–
	Day 40	+	+/–	+	–	–	–
STSG-E	Day 40	+	+/–	+/–	+	–	–
STSG-SPD	Day 40	+	++	++	+	–	+/–

E – epidermis, SPD – *stratum papilare dermis*, SCT – subcutaneous tissue

Table 3. Semi-quantitative expression of immunostained structures/markers in bioptic samples removed from areas covered by Integra® dermal template and split-thickness skin graft (STSG)

		Vim	CD31	CD34	SMA	Ki67	Bcl-2	p53
Integra®	Day 7	++	+/–	+/–	–	–	–	–
	Day 10	++	+/–	+/–	++	+	–	–
	Day 21	+++	+	+	++	+	–	–
	Day 40	+++	+	+	+	+	+	+
SCT	Day 7	+++	++	++	+	+	+/–	–
	Day 10	+++	+	+	+++	++	+/–	+/–
	Day 21	+++	++	++	+	+	–	–
	Day 40	+++	+	+	+	–	–	+
STSG-E	Day 40	+	–	–	–	++	+	++
STSG-SPD	Day 40	+++	++	++	+++	++	–	+

E – epidermis, SPD – *stratum papilare dermis*, SCT – subcutaneous tissue

Table 4. Semi-quantitative expression of epithelial structures/markers in bioptic samples removed from areas covered by Integra® dermal template and split-thickness skin graft (STSG)

		p63	K14	K19	E-Cad
STSG-E	Day 40	+++	+++	–	+++
STSG-SPD	Day 40	–	–	–	–

E – epidermis, SPD – *stratum papilare dermis*

was expressed by deposition of extracellular matrix and production of granulation-like tissue. Thus, the Sirius red staining and polarized light microscopy clearly demonstrated that the artificial template was gradually filled with newly formed tissue, which was only poorly seen on days 7 and 10.

The STSG (applied on day 33) contained papillary dermis and an intact epidermal layer with proliferating (Ki67-positive) basal epidermal layer and normal stratification (Fig. 5). The characteristic structure of papillary dermis could be observed, and luminized vessels ensuring nutrition for the STSG were already present (Fig. 4).

Immunophenotype of the dermal template and STSG

The presence of immunity-related cells in the investigated tissue layers was confirmed by staining with LCA (CD45) (Table 2). Moreover, this staining also showed an increase in the number of immune cells on days 7 and 10 in the SCT and on day 10 also in the Integra® template (Fig. 3). Staining of the artificial dermis with the CD3 marker showed a gradual increase in T-cell numbers from day 7 to day 40. The population of $CD4^+$ T cells, which was weakly positive on day 7, expanded progressively over the course of the study. On the other hand, the population of $CD8^+$ T cells was found positive in the Integra® template only on day 40. In contrast, op-

posite dynamics of $CD8^+$ cells was observed in the SCT when compared to the Integra® template. $CD3^+$ T-cell numbers were kept steady until day 40, when a decrease in their numbers was observed. The population of $CD4^+$ T cells decreased over the course of the study, but remained positive in SCT. Moreover, the $CD8^+$ T cells observed on days 7 and 10 in SCT were not present on days 21 and 40. Comparing each of the studied layers on day 40, the $CD4^+$ T-cell population was found in each of the layers except for the STSG-E layer, which was rather CD4 negative. A CD8 T-cell population was found in each layer except the SCT. Of note, the investigated tissue layers were CD56 and CD57 negative, manifesting no/weak NK cell infiltration.

Discussion

To the best of our knowledge, our study represents the first insight into the immune system response related to Integra® application in a severely burned human patient. In detail, the immunohistochemical investigation of the artificial dermis revealed that immune cell infiltration reaches its peak on day 10, three days later when compared to the subcutaneous tissue, which correlates with Phase II of burn repair with artificial skin (Stern et al., 1990). The tissue immunophenotype found an increase in $CD3^+$ cells over the course of the study as well as CD4 and CD8 positivity on day 40, indicating remaining T-cell subpopulations. On the other hand, subcutaneous tissue was CD3 as well as CD4 and CD8 negative on day 40. Considering that T cells are a key immune system player responsible for graft rejection (Anderson et al., 2008; Dixit et al., 2017), such finding supports the hypothesis of unresolved inflammation present in Integra®, supporting previous findings showing weak immunogenic potential of this template, most probably due to its non-human, but bovine, origin (Jones et al., 2002). We observed weak/no infiltration of NK cells ($CD56^+$), which was rather expected as these cells play a crucial role in virus-infected and neoplastic cell elimination (Mandal and Viswanathan, 2015).

Formation of the granulation tissue appeared to proceed more slowly than in normal open wounds (Gal et al., 2008; Shestakova et al., 2020). However, the newly formed collagen was similar to normal collagen of intact skin (Stern et al., 1990; Muangman et al., 2006). Similarly, as seen previously (Moiemen et al., 2006), we observed no signs of pathological scaring, such as the presence of thick collagen bundles or nodules typical of keloids or hypertrophic scars, respectively (Ghazawi et al., 2018). Long-term (ranging from 35 months to 14 years) histological analysis confirmed the trend of normal collagen arrangement (Moiemen et al., 2011; Zajicek et al., 2018). On the other hand, the elastic fibres were also found in the regenerated template, however, of a rather abnormal and reduced density and more irregular distribution (Moiemen et al., 2011). Furthermore, we did not observe formation of any skin adnexa.

In conclusion, the use of bi-layer Integra® represents a feasible and safe procedure resulting in formation of non-irritating dermal substitutes. Although we analysed several markers of immune cells, other lymphocytes such as B cells and various $CD4^+$ T-cell subpopulations were not investigated in this study due to immunohistochemical co-staining limitations, which present a limitation of our study. In particular, identification of $CD4^+$ T-cell subsets may help elucidate the Th1/Th2 immune response polarization. Therefore, further in-depth studies conducted on a higher number of human subjects and analysis of other immune cell subpopulations, particularly neutrophils and monocytes, are required to complete the immune profile of Integra® and to fully understand the immunity-related processes during skin regeneration using this template.

Conflict of interest

The authors have no conflict of interest to declare.

Acknowledgements

We thank Professor Karel Smetana Jr. for critically reading the article and for his useful comments. Authors are also grateful to J. Kosorínová for her great technical assistance.

References

Anderson, J. M., Rodriguez, A., Chang, D. T. (2008) Foreign body reaction to biomaterials. *Semin. Immunol.* **20**, 86-100.

Auxenfans, C., Menet, V., Catherine, Z., Shipkov, H., Lacroix, P., Bertin-Maghit, M., Damour, O., Braye, F. (2015) Cultured autologous keratinocytes in the treatment of large and deep burns: a retrospective study over 15 years. *Burns* **41**, 71-79.

Burke, J. F., Yannas, I. V., Quinby, W. C., Bondoc, C. C., Jung, W. K. (1981) Successful use of a physiologically acceptable artificial skin in the treatment of extensive burn injury. *Ann. Surg.* **194**, 413-428.

Capito, A. E., Tholpady, S. S., Agrawal, H., Drake, D. B., Katz, A. J. (2012) Evaluation of host tissue integration, revascularization, and cellular infiltration within various dermal substrates. *Ann. Plast. Surg.* **68**, 495-500.

Cheshire, P. A., Herson, M. R., Cleland, H., Akbarzadeh, S. (2016) Artificial dermal templates: A comparative study of NovoSorb (TM) biodegradable temporising matrix (BTM) and Integra (R) dermal regeneration template (DRT). *Burns* **42**, 1088-1096.

Dagalakis, N., Flink, J., Stasikelis, P., Burke, J. F., Yannas, I. V. (1980) Design of an artificial skin. 3. Control of pore structure. *J. Biomed. Mater. Res.* **14**, 511-528.

Dixit, S., Baganizi, D. R., Sahu, R., Dosunmu, E., Chaudhari, A., Vig, K., Pillai, S. R., Singh, S. R., Dennis, V. A. (2017) Immunological challenges associated with artificial skin grafts: available solutions and stem cells in future design of synthetic skin. *J. Biol. Eng.* **11**, 49.

Dunkin, C. S. J., Pleat, J. M., Gillespie, P. H., Tyler, M. P. H., Roberts, A. H. N., McGrouther, D. A. (2007) Scarring occurs at a critical depth of skin injury: precise measurement

in a graduated dermal scratch in human volunteers. *Plast. Reconstr. Surg.* **119**, 1722-1732.

Gal, P., Kilik, R., Mokry, M., Vidinsky, B., Vasilenko, T., Mozes, S., Bobrov, N., Tomori, Z., Bober, J., Lenhardt, L. (2008) Simple method of open skin wound healing model in corticosteroid-treated and diabetic rats: standardization of semi-quantitative and quantitative histological assessments. *Vet. Med.* **53**, 652-659.

Ghazawi, F. M., Zargham, R., Gilardino, M. S., Sasseville, D., Jafarian, F. (2018) Insights into the pathophysiology of hypertrophic scars and keloids: how do they differ? *Adv. Skin Wound Care* **31**, 582-594.

Grant, I., Green, C., Martin, R. (2001) Strategies to improve the take of commercially available collagen/glycosaminoglycan wound repair material investigated in an animal model. *Burns* **27**, 699-707.

Haertsch, P. (2002) Reconstructive surgery using an artificial dermis (Integra). *Br. J. Plast. Surg.* **55**, 362-363.

Heimbach, D. M., Warden, G. D., Luterman, A., Jordan, M. H., Ozobia, N., Ryan, C. M., Voigt, D. W., Hickerson, W. L., Saffle, J. R., DeClement, F. A., Sheridan, R. L., Dimick, A. R. (2003) Multicenter postapproval clinical trial of Integra dermal regeneration template for burn treatment. *J. Burn Care Rehabil.* **24**, 42-48.

Jones, I., Currie, L., Martin, R. (2002) A guide to biological skin substitutes. *Br. J. Plast. Surg.* **55**, 185-193.

Kanapathy, M., Hachach-Haram, N., Bystrzonowski, N., Harding, K., Mosahebi, A., Richards, T. (2016) Epidermal grafting versus split-thickness skin grafting for wound healing (EPIGRAAFT): study protocol for a randomised controlled trial. *Trials* **17**, 245.

King, W. W., Lam, P. K., Liew, C. T., Ho, W. S., Li, A. K. (1997) Evaluation of artificial skin (Integra) in a rodent model. *Burns* **23(Suppl 1)**, S30-32.

Mandal, A., Viswanathan, C. (2015) Natural killer cells: In health and disease. *Hematol. Oncol. Stem Cell Ther.* **8**, 47-55.

Moiemen, N. S., Vlachou, E., Staiano, J. J., Thawy, Y., Frame, J. D. (2006) Reconstructive surgery with Integra dermal regeneration template: histologic study, clinical evaluation, and current practice. *Plast. Reconstr. Surg.* **117**, 160S-174S.

Moiemen, N., Yarrow, J., Hodgson, E., Constantinides, J., Chipp, E., Oakley, H., Shale, E., Freeth, M. (2011) Long-term clinical and histological analysis of Integra dermal regeneration template. *Plast. Reconstr. Surg.* **127**, 1149-1154.

Muangman, P., Deubner, H., Honari, S., Heimbach, D. M., Engrav, L. H., Klein, M. B., Gibran, N. S. (2006) Correlation of clinical outcome of Integra application with microbiologic and pathological biopsies. *J. Trauma* **61**, 1212-1217.

Nguyen, D. Q., Potokar, T. S., Price, P. (2010) An objective long-term evaluation of Integra (a dermal skin substitute) and split thickness skin grafts, in acute burns and reconstructive surgery. *Burns* **36**, 23-28.

Shaterian, A., Borboa, A., Sawada, R., Costantini, T., Potenza, B., Coimbra, R., Baird, A., Eliceiri, B. P. (2009) Real-time analysis of the kinetics of angiogenesis and vascular permeability in an animal model of wound healing. *Burns* **35**, 811-817.

Shestakova, V. G., Nikityuk, D. B., Bazhenov, D. V., Banin, V. V. (2020) Relationship of structural and tissue components of full-layer skin wound and mathematical modeling of the healing process. *Bull. Exp. Biol. Med.* **169**, 401-404.

Stern, R., McPherson, M., Longaker, M.T. (1990) Histologic study of artificial skin used in the treatment of full-thickness thermal injury. *J. Burn. Care Rehabil.* **11**, 7-13.

Varkey, M., Ding, J., Tredget, E. E. (2015) Advances in skin substitutes – potential of tissue engineered skin for facilitating anti-fibrotic healing. *J. Funct. Biomater.* **6**, 547-563.

Yannas, I. V., Burke, J. F. (1980) Design of an artificial skin. 1. Basic design principles. *J. Biomed. Mater. Res.* **14**, 65-81.

Yannas, I. V., Burke, J. F., Gordon, P. L., Huang, C., Rubenstein, R. H. (1980) Design of an artificial skin. 2. Control of chemical composition. *J. Biomed. Mater. Res.* **14**, 107-132.

Yannas, I. V., Burke, J. F., Warpehoski, M., Stasikelis, P., Skrabut, E. M., Orgill, D., Giard, D. J. (1981) Prompt, long-term functional replacement of skin. *Trans. Am. Soc. Artif. Inter. Organs* **27**, 19-23.

Yannas, I. V., Lee, E., Orgill, D. P., Skrabut, E. M., Murphy, G. F. (1989) Synthesis and characterization of a model extracellular matrix that induces partial regeneration of adult mammalian skin. *Proc. Natl. Acad. Sci. USA* **86**, 933-937.

Zajicek, R., Sticova, E., Konigova, R. (2018) A histological analysis of artificial skin in an extensively burned child, 14 years after application: a case report. *J. Wound Care* **27**, 14-18.